

# PEG Brush Peptide Nanospheres with Stealth Properties and Chemical Functionality

Tomonori Waku,<sup>†</sup> Michiya Matsusaki,<sup>†</sup> Tatsuo Kaneko,<sup>†,§</sup> and Mitsuru Akashi<sup>\*,†,‡</sup>

Department of Applied Chemistry, Graduate School of Engineering, Osaka University, 2-1 Yamada-oka, Suita 565-0871, Japan, and Core Research for Evolutional Science and Technology (CREST), Japan Science and Technology Agency (JST), 4-1-8 Honcho, Kawaguchi-shi 332-0012, Japan

Received March 30, 2007; Revised Manuscript Received June 11, 2007

**ABSTRACT:** Peptide nanospheres with PEG brushes were prepared by the one-step polymerization of L-phenylalanine (Phe) *N*-carboxyanhydride with the dual initiators of hydrophobic *n*-butylamine and hydrophilic NH<sub>2</sub>-monoterminated PEG (NH<sub>2</sub>-PEG). We successfully prepared peptide nanospheres with CH<sub>3</sub>O or COOH groups using CH<sub>3</sub>O- or COOH-terminated PEG as one of the initiators. The high-density PEG brush conformation of the peptide nanospheres was confirmed by <sup>1</sup>H NMR measurements. FT-IR measurements suggested closely packed Phe polymer chains in the core in a  $\beta$ -strand conformation. The results of protein adsorption experiments onto both nanosphere surfaces indicated that PEG-brush corona layers inhibited nonspecific protein adsorption, even in Eagle's medium (10% FBS). Furthermore, target proteins were covalently immobilized onto the surface of the COOH-PEG peptide nanospheres by amide bond formation. Peptide nanospheres with PEG brushes may be useful as novel nanospheres possessing both stealth properties and chemical functionality for drug delivery systems and biological diagnosis.

## Introduction

Nanospheres have been widely studied since they are promising carriers for drugs, genes, proteins, and antigens.<sup>1–7</sup> We have vigorously studied various self-assembling synthetic<sup>8,9</sup> and biodegradable<sup>10–12</sup> nanospheres and hollow capsules<sup>13,14</sup> for biomedical applications such as a drug delivery system (DDS) and diagnosis. For the successful targeted delivery of drugs or proteins using nanospheres, it is necessary that the nanospheres have bioinert surfaces, which can inhibit the nonspecific adsorption of serum proteins and hemocytes in order to maintain their stable circulation and property in the blood without being scavenged nonselectively.<sup>1,15</sup> Recently, the development of bioinert surfaces, the preparation of polymer brushes on the surface of solid substrates, has attracted much attention.<sup>16–18</sup> Some researchers reported core–shell type nanospheres coated with polymer brushes, which were synthesized by multistep preparations such as an atom transfer radical polymerization (ATRP) initiated from the surface of silica seed particles modified with initiators.<sup>19–21</sup> However, this method has a limitation in the biomedical field because ATRP can prepare only nanospheres composed of vinyl polymers without biocompatibility or biodegradability. Furthermore, the degradability of the component polymers to innocuous monomers should enable excretion through the kidneys due to the polymer size and their hydrophilicity.<sup>15</sup> As far as we know, there have been no reports of nanospheres composed of biodegradable solid cores with biocompatible polymer brushes. On the other hand, the chemical functionality of the nanospheres is also significant to immobilize target drugs or proteins onto their surface for target disease specificity. Thus, biodegradable nanospheres possessing biocompatible polymer brushes and the capability for chemical

modification of their surface with target molecules are very useful for biomedical applications.

Recently, we reported a novel method for the preparation of surface-grafted peptide nanospheres consisting of hydrophobic poly(phenylalanine) (PPhe) with hydrophilic poly(ethylene glycol) (PEG) grafts.<sup>22</sup> The peptide nanospheres were successfully synthesized by the one-step polymerization of L-phenylalanine *N*-carboxyanhydride (Phe-NCA) with the dual initiators of hydrophobic *n*-butylamine and hydrophilic NH<sub>2</sub>-monoterminated PEG (NH<sub>2</sub>-PEG), exploiting the self-assembling process with hydrophobic interactions of the Phe segments (Scheme 1). These nanospheres with a biodegradable solid core are expected to possess the special advantage of stability without dissociation after dilution in body fluids, unlike a polymer micelle consisting of amphiphilic block copolymer.<sup>23</sup> These peptide nanospheres have a diameter of ~300 nm, suggesting the favorable covalent immobilization of a wide range of target macromolecules from a few nanometers to several tens of nanometers in size such as peptides, proteins, and antigens. In addition, in our method, various combinations of monomers and initiators will enable the preparation of a variety of peptide nanospheres with different surfaces and core structures.

In the present study, we investigated the PEG chain densities on the surface of peptide nanospheres by <sup>1</sup>H NMR measurements. The PEG densities were approximately 0.21–1.8 chains/nm<sup>2</sup>, depending on the molecular weight of the PEG initiators (*M*<sub>w</sub> = 2000–4500), indicating a high-density regime of PEG brushes. Such high-density polymer brushes have been successfully prepared only by surface-initiated living radical polymerization. Interestingly, peptide nanospheres with high-density PEG brushes were generated successfully by the one-step polymerization of NCA initiated by dual initiators. FT-IR analyses of the secondary structure of the core in the peptide nanospheres clarified the relationship between the close packing PEG chains and the  $\beta$ -strand conformation of Phe segments. Furthermore, nonspecific protein adsorption was completely inhibited, even in Eagle's medium containing 10% fetal bovine

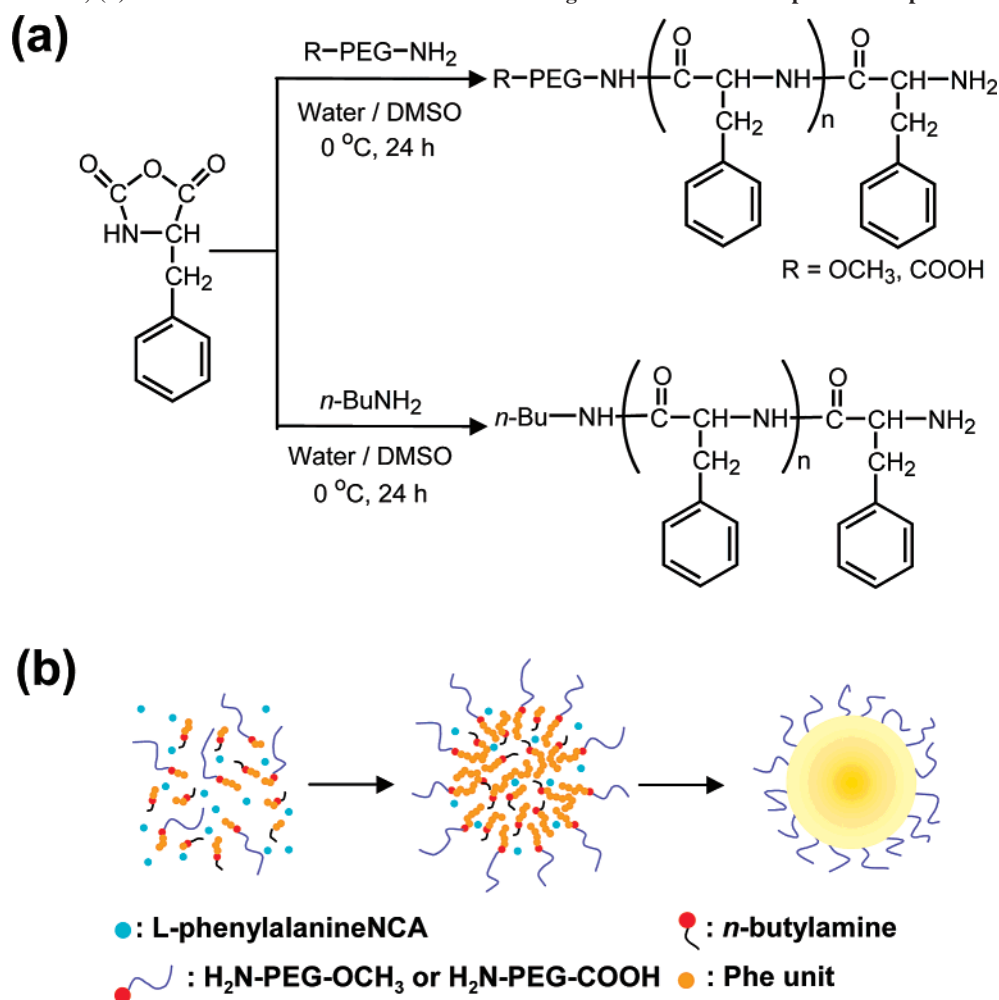
\* To whom correspondence should be addressed: Tel +81-6-6879-7356; Fax +81-6-6879-7359; e-mail akashi@chem.eng.osaka-u.ac.jp.

<sup>†</sup> Osaka University.

<sup>‡</sup> Japan Science and Technology Agency.

<sup>§</sup> Current affiliation: School of Materials Science, Japan Advanced Institute of Science and Technology, 1-1 Asahidai, Nomi, Ishikawa 923-1292, Japan.

**Scheme 1.** (a) Synthesis of Peptide Nanospheres Composed of Hydrophobic Poly(phenylalanine) with Hydrophilic Poly(ethylene glycol) Grafts; (b) Schematic Illustration of the Self-Assembling Mechanism of the Peptide Nanospheres<sup>22</sup>



serum, and amide bond formation between the terminal carboxyl group of the PEG corona layers and the amino group of proteins enabled the immobilization of the target proteins. Thus, these biodegradable peptide nanospheres that can avoid nonspecific protein adsorption (their stealth properties) plus chemical functionality can be useful as a novel drug carrier for DDS and biological diagnosis.

## Experimental Section

**Materials.** L-Phenylalanine (Phe), tetrahydrofuran (THF), *n*-hexane, dimethyl sulfoxide (DMSO), and 1-ethyl-3-(3-(dimethylamino)propyl)carbodiimide (WSC) were purchased from Wako Pure Chemical Industries (Japan) and were used without further purification unless otherwise noted. THF and *n*-hexane were distilled over sodium before use. DMSO was distilled over calcium hydride before use. Triphosgene was purchased from Tokyo Chemical Industry Corp. (Japan) and used as received. *n*-Butylamine was purchased from Kishida Chemical Corp. (Japan) and used without purification.  $\alpha$ -Aminopropyl- $\omega$ -methoxypolyoxyethylene (NH<sub>2</sub>-PEG-OCH<sub>3</sub>;  $M_w$  is 2000, 5000, 12 000, and 20 000) and  $\alpha$ -aminopropyl- $\omega$ -carboxypolyoxyethylene, polyoxyethylene, hydrochloride (HCl•NH<sub>2</sub>-PEG-COOH;  $M_w$  is 2000, 3400, and 4500) were purchased from NOF Corp. (Japan), and used as received. Bovine serum albumin (BSA), ovalbumin (OVA), lysozyme, and cytochrome *c* were purchased from Sigma (St. Louis, MO).

**Synthesis of Phe-NCA.** Phe-NCA was prepared according to the previously reported method.<sup>24,25</sup> Phe-NCA was synthesized by the reaction of L-phenylalanine (60.6 mmol) with triphosgene (20.2 mmol) in THF (200 mL) for 4 h at 45 °C and purified by subsequent reprecipitation in *n*-hexane. The yield was 77%.

**Peptide Nanosphere Preparation.** The preparation of representative peptide nanospheres using NH<sub>2</sub>-PEG-OCH<sub>3</sub> as an initiator (Table 1, run 4) was performed as follows.<sup>22</sup> Briefly, 310  $\mu$ mol of Phe-NCA was dissolved in 150  $\mu$ L of DMSO at room temperature under a nitrogen atmosphere and 26  $\mu$ mol of NH<sub>2</sub>-PEG-OCH<sub>3</sub> ( $M_w$  = 2000) and *n*-butylamine (BA) as initiators were dissolved in water/DMSO (4 mL/850  $\mu$ L) at 0 °C. The DMSO solution containing Phe-NCA was gently dropped into the water/DMSO containing NH<sub>2</sub>-PEG-OCH<sub>3</sub> and BA, and then the reaction mixture was stirred at 0 °C for 24 h. After the reaction, the obtained nanospheres were purified by dialysis (Spectra/Pore membrane, 50 000 molecular weight cutoff) in distilled water for 3 days. The particles were then centrifuged and redispersed in water.

**Preparation of Surface-Functional Peptide Nanospheres.** Surface functional peptide nanospheres were prepared using NH<sub>2</sub>-PEG-COOH as an initiator (Table 1, run 16) as follows. 26  $\mu$ mol of NH<sub>2</sub>-PEG-COOH ( $M_w$  = 2000) and BA as initiators was dissolved in water. The pH of the initiator solution was adjusted to 10.7 with 1 N NaOH, and then 850  $\mu$ L of DMSO was added into the solution. Phe-NCA (310  $\mu$ mol) in 150  $\mu$ L of DMSO was gently dropped into the water/DMSO containing both initiators, and then the reaction solution was stirred at 0 °C for 24 h. The nanospheres were purified by dialysis (Spectra/Pore membrane, 50 000 molecular weight cutoff) in distilled water for 3 days, and the obtained particles were centrifuged and redispersed in water.

**Measurements.** <sup>1</sup>H NMR spectra of the peptide nanospheres were measured with a JNM-GSX-400 spectrometer (400 MHz; JEOL, Japan) using a chloroform-*d*/trifluoroacetic acid (TFA)-*d* mixed solvent (chloroform-*d*/TFA-*d* = 4/1 v/v) for the composition analysis of the peptide nanospheres and D<sub>2</sub>O for estimating the PEG chain densities on the nanosphere surface. Attenuated total

Table 1. Synthesis and Characterization of the PEG Brush Peptide Nanospheres<sup>a</sup>

| run no. | Phe-NCA (mmol/L) | initiators                        |                           |                          | feed ratio (NCA:PEG:BA) | solvent (water:DMSO) | $d_m^d$ (nm) | CV <sup>e</sup> (%) | yield (%) | sphere formation |
|---------|------------------|-----------------------------------|---------------------------|--------------------------|-------------------------|----------------------|--------------|---------------------|-----------|------------------|
|         |                  | PEG <sup>b</sup> struct ( $M_w$ ) | PEG <sup>b</sup> (mmol/L) | BA <sup>c</sup> (mmol/L) |                         |                      |              |                     |           |                  |
| 1       | 63               | PEG-OCH <sub>3</sub> (2K)         | 0                         | 5.3                      | 12:0:1                  | 80:20                |              |                     | 69        | ×                |
| 2       | 63               | PEG-OCH <sub>3</sub> (2K)         | 2.7                       | 5.3                      | 12:0.5:1                | 80:20                |              |                     | 75        | ×                |
| 3       | 63               | PEG-OCH <sub>3</sub> (2K)         | 5.3                       | 11                       | 12:1:2                  | 80:20                |              |                     | 39        | ×                |
| 4       | 63               | PEG-OCH <sub>3</sub> (2K)         | 5.3                       | 5.3                      | 12:1:1                  | 80:20                | 430          | 26                  | 40        | ○                |
| 5       | 63               | PEG-OCH <sub>3</sub> (2K)         | 11                        | 5.3                      | 12:2:1                  | 80:20                |              |                     | 26        | ×                |
| 6       | 63               | PEG-OCH <sub>3</sub> (2K)         | 5.3                       | 2.7                      | 12:1:0.5                | 80:20                | 190          | 20                  | 64        | △                |
| 7       | 63               | PEG-OCH <sub>3</sub> (2K)         | 5.3                       | 0                        | 12:1:0                  | 80:20                |              |                     | ×         | ×                |
| 8       | 63               | PEG-OCH <sub>3</sub> (2K)         | 5.3                       | 5.3                      | 12:1:1                  | 95:5                 | 250          | 26                  | 41        | ○                |
| 9       | 63               | PEG-OCH <sub>3</sub> (2K)         | 5.3                       | 5.3                      | 12:1:1                  | 90:10                | 310          | 28                  | 33        | ○                |
| 10      | 63               | PEG-OCH <sub>3</sub> (2K)         | 5.3                       | 5.3                      | 12:1:1                  | 80:20                | 430          | 26                  | 40        | ○                |
| 11      | 63               | PEG-OCH <sub>3</sub> (2K)         | 5.3                       | 5.3                      | 12:1:1                  | 60:40                |              |                     | 38        | ×                |
| 12      | 63               | PEG-OCH <sub>3</sub> (2K)         | 5.3                       | 5.3                      | 12:1:1                  | 20:80                |              |                     | 52        | ×                |
| 13      | 63               | PEG-OCH <sub>3</sub> (5K)         | 2.1                       | 2.1                      | 30:1:1                  | 80:20                | 350          | 28                  | 51        | ○                |
| 14      | 63               | PEG-OCH <sub>3</sub> (12K)        | 0.88                      | 0.88                     | 72:1:1                  | 80:20                | 350          | 29                  | 66        | ○                |
| 15      | 63               | PEG-OCH <sub>3</sub> (20K)        | 0.53                      | 0.53                     | 120:1:1                 | 80:20                | 380          | 25                  | 50        | ○                |
| 16      | 63               | PEG-COOH (2K)                     | 5.3                       | 5.3                      | 12:1:1                  | 80:20                | 380          | 25                  | 67        | ○                |
| 17      | 63               | PEG-COOH (3.4K)                   | 3.1                       | 3.1                      | 20:1:1                  | 80:20                | 340          | 30                  | 33        | ○                |
| 18      | 63               | PEG-COOH (4.5K)                   | 2.4                       | 2.4                      | 26:1:1                  | 80:20                | 210          | 29                  | 22        | ○                |

<sup>a</sup> Reaction time was 24 h, and temperature was 0 °C. The data of runs 1–3, 5–9, 11, and 12 were the same condition in ref 22. <sup>b</sup> PEG is poly(ethylene glycol) monoterminated with amino groups. <sup>c</sup> BA is *n*-butylamine. <sup>d</sup> Mean diameter was measured by dynamic laser scattering (DLS). <sup>e</sup> CV is SD/ $d_m$ ; coefficient of variation.

reflection (ATR) infrared spectra of the nanospheres were obtained with a Spectrum One FT-IR spectrometer (Perkin-Elmer). The interferograms were coadded 16 times and Fourier-transformed at a resolution of 4 cm<sup>-1</sup>. Scanning electron microscope (SEM) images were obtained with a JSM-6700F (JEOL, Japan). The particle size distribution and  $\zeta$  potential of the peptide nanospheres in aqueous solution were measured by a dynamic light scattering (DLS) method using a Zetasizer Nano ZS (Malvern Instruments, UK). Electron spectroscopy for chemical analysis (ESCA) was performed with a ESCA 1000 (Shimadzu, Japan) employing Mg K $\alpha$  radiation (1253.6 eV) and a pass energy of 31.5 eV. X-ray diffraction (XRD) patterns were taken with a Geigerflex RAD-II B (Rigaku, Japan) emitting Ni-filtered Cu K $\alpha$  radiation (30 kV, 15 mA) at scanning angles ranging from 35° to 5° at a scanning rate of 2° min<sup>-1</sup>.

**Structural Analyses of Peptide Nanospheres.** <sup>1</sup>H NMR Measurements of the Peptide Nanospheres. We estimated the number of PEG chains on the surface of the peptide nanospheres from the PEG methylene peak at 3.5–3.7 ppm vs the methyl proton peak of sodium 2,2-dimethyl-2-silapentane-5-sulfonate (DSS) as an internal standard at 0 ppm.

**FT-IR Measurement of the Peptide Nanospheres.** 310  $\mu$ mol of Phe-NCA was dissolved in 150  $\mu$ L of DMSO-*d*<sub>6</sub> at room temperature, and 26  $\mu$ mol of NH<sub>2</sub>-PEG-OCH<sub>3</sub> ( $M_w$  = 2000) and *n*-butylamine (BA) as initiators was dissolved in D<sub>2</sub>O/DMSO-*d*<sub>6</sub> (8 mL/1.85 mL) at 0 °C. The DMSO containing Phe-NCA was gently dropped into the water/DMSO containing both initiators, and then the reaction mixture was stirred at 0 °C for 24 h. The secondary structure of the core in the peptide nanospheres related to the polymerization time was analyzed by their FT-IR spectra. During the polymerization process, the nanospheres were collected after prescribed times (0.5, 1, 2, 8, and 24 h) by centrifugation, and their FT-IR spectra were measured without a drying process.

**Physical Adsorption or Chemical Immobilization of Proteins onto the Peptide Nanospheres. Physical Adsorption of Proteins.** The peptide nanospheres were dispersed in phosphate buffered saline (PBS, pH 7.4) at 10 mg/mL and incubated with an equivalent volume of 4 mg/mL protein solutions (PBS, pH 7.4) at 4 °C for 24 h. The nanospheres were isolated by centrifugation and washed twice with PBS. The amount of adsorbed proteins on the peptide nanospheres was determined by the ninhydrin method after hydrolyzing the adsorbed proteins with 2.5 N HCl at 100 °C for 2 h. The peptide nanospheres were stable under these hydrolysis conditions. The original peptide nanospheres without the protein adsorption process were used as a control, and calibration curves were prepared from each protein at various concentrations. The ninhydrin test was performed as follows. Briefly, nanospheres after

the protein adsorption process were added to 2.5 N HCl at 100 °C for 2 h to hydrolyze the amide bond of the protein. The reaction solution was neutralized with NaOH and filtered through a 0.22  $\mu$ m filter, and 0.5% (w/v) ninhydrin, 0.075% (w/v) hydrindantin, 20% (v/v) 2-methoxyethanol, and 0.25 M sodium acetate (pH 5.5) were added to the solution. The absorbance at 570 nm was measured with a microplate reader. Using a calibration curve for a reference protein, the amount of immobilized proteins per cm<sup>2</sup> was estimated.

**Chemical Immobilization of Proteins.** The peptide nanospheres were dispersed in phosphate buffer (PB, pH 5.8) at 10 mg/mL and mixed with an equivalent volume of 2 mg/mL WSC solution in PB (pH 5.8). The mixture was incubated at 4 °C for 20 min. Then, the nanospheres were isolated by centrifugation and redispersed in PBS at 10 mg/mL. This dispersion solution was mixed with an equivalent volume of 4 mg/mL of protein solution in PBS (pH 7.4) and incubated at 4 °C for 24 h. The nanospheres were then isolated by centrifugation, washed twice with PBS, and redispersed at 5 mg/mL. The amount of immobilized proteins was subsequently determined by the above-mentioned ninhydrin method.

## Results and Discussion

**Preparation of the Peptide Nanospheres.** As shown in the previous paper,<sup>22</sup> the peptide nanospheres were synthesized by the polymerization of L-phenylalanine *N*-carboxyanhydride (Phe-NCA) with the dual initiators of hydrophobic *n*-butylamine and hydrophilic NH<sub>2</sub>-monoterminated PEG (NH<sub>2</sub>-PEG). In this dual initiators method, the peptide nanospheres are formed by self-organization of the two growing polymers: hydrophobic Phe homopolymers and amphiphilic p(Phe-*b*-EG) copolymer via hydrophobic interactions of the Phe segments. We anticipated that the composition ratios of the obtained polymers, PPhe and p(Phe-*b*-EG), would strongly influence the nanospheres formation behavior, and thus we evaluated the effects of the initiators during nanosphere formation. Phe-NCA was polymerized with various feed ratios of NH<sub>2</sub>-PEG-OCH<sub>3</sub> and BA in DMSO/water (1/4 v/v) at 0 °C for 24 h (Table 1, runs 1–7). In all cases, suspensions were obtained after the polymerization, and thus the reaction solutions were substituted with ultrapure water through the dialysis process. The morphology and diameter of the obtained samples were analyzed by SEM observations and DLS measurements, respectively. When the feed molar ratio of NCA:PEG:BA was 12:1:1 (Table 1, run 4), spheres with a diameter of about 430 nm were formed (Figure 1a). However,



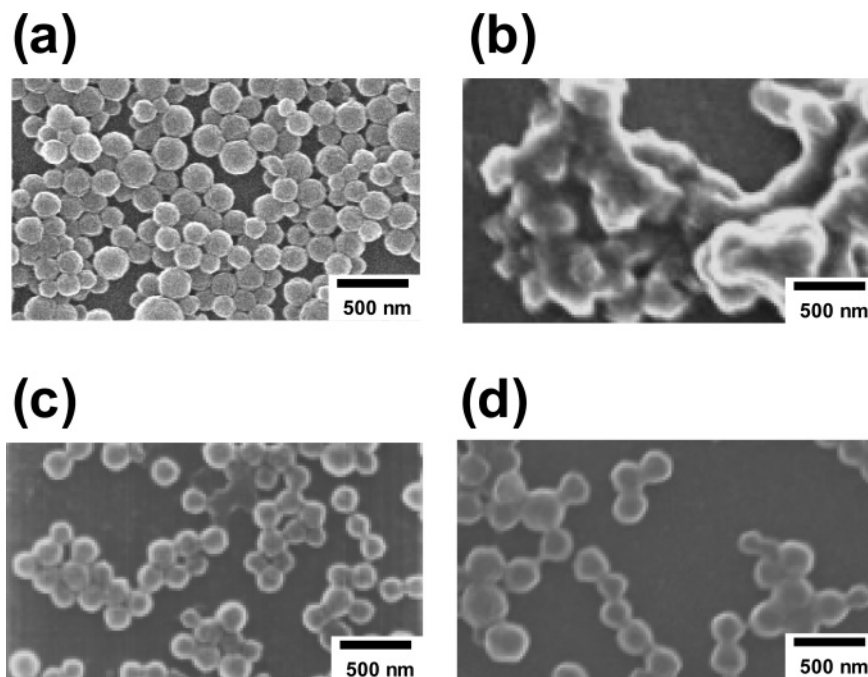


**Figure 1.** Scanning electron microscopic (SEM) images of nanospheres composed of hydrophobic poly(phenylalanine) with hydrophilic poly(ethylene glycol) grafts. (a) and (b) were prepared with  $\text{NH}_2\text{-PEG-OCH}_3$  (2K) as one of the initiators. (a) The feed ratio of NCA:PEG:BA was 12:1:1 (Table 1, run 4), and (b) the feed ratio of NCA:PEG:BA was 12:2:1 (Table 1, run 3). (c) was prepared with  $\text{NH}_2\text{-PEG-OCH}_3$  (20K), and the feed ratio of NCA:PEG:BA was 120:1:1 (Table 1, run 15). (d) was prepared with  $\text{NH}_2\text{-PEG-COOH}$  (2K), and the feed ratio of NCA:PEG:BA was 12:1:1 (Table 1, run 16).

nanosphere formation was not observed in the other cases. When the PEG/BA ratio was smaller than 1.0 (Table 1, runs 1–3), only aggregates were observed, as shown in Figure 1b. We speculated that these phenomena were caused by an inability of the hydrophilic PEG chains to stabilize the hydrophobic core composed of PPhe and Phe segments of p(Phe-*b*-EG). However, when the PEG/BA ratio was larger than 1.0 (Table 1, runs 5–7), the SEM observations also did not show any nanosphere formation, but the DLS histogram indicated a single peak (run 6), indicating nanosphere formation. The discrepancy between the SEM observations and the DLS measurements were likely due to inadequate hydrophobicity of the core during the drying process for SEM measurements. Therefore, we concluded that the composition ratios of PPhe and p(Phe-*b*-EG) strongly affected nanosphere formation and stability. The hydrophilic–hydrophobic balance between the hydrophobic core and the hydrophilic corona layer is significant, and the in feed molar ratio of Phe-NCA and initiators is important for the nanosphere formation. When the Phe-NCA was polymerized at the condition of NCA:PEG:BA = 12:0.5:0.5, the peptide nanospheres with a diameter of about 290 nm were observed, although the nanosphere formation was not observed at the condition of NCA:PEG:BA = 12:0.24:0.24. These results suggest that the appropriate molar ratio of NCA:PEG:BA is 12:0.5–1.0:0.5–1.0.

We then evaluated the solvent effect for nanosphere formation. Phe-NCA was polymerized in a DMSO/water mixed solvent of various compositions: water content of 95, 90, 80, 60, and 20 vol %, at 0 °C for 24 h. In the water composition range from 80 to 95 vol %, the nanospheres were successfully formed (Table 1, runs 8–10). The sizes of the obtained nanospheres were 250–430 nm, and the CV values were 26–28%. On the other hand, in the water composition range from 20 to 60 vol %, SEM observations and DLS measurements showed only aggregations (Table 1, runs 11 and 12). These results suggested instability of the core due to weak hydrophobic interactions in the DMSO-rich aqueous solution.

In our previous study, we reported that  $^1\text{H}$  NMR measurements showed the localization of PEG chains on the nanosphere surfaces.<sup>22</sup> We anticipated the ability to control the surface structures on the nanospheres, such as the length of the graft chains and the presence or absence of functional groups, by altering the structure of the PEG macroinitiator. We performed the synthesis of peptide nanospheres using PEG macroinitiators of different molecular weights such as 5000, 12 000, and 20 000. The polymerization conditions and characterization of the obtained peptide nanospheres are listed in Table 1, runs 13–15. In all cases, nanosphere formation was confirmed by SEM observations and DLS measurements (Figure 1c). The yields were 50–66%, and the sizes of the nanospheres were 350–380 nm. We also attempted to synthesize peptide nanospheres with carboxylic groups on the surface by using  $\text{HOOC-PEG-NH}_2$  with different molecular weights as an initiator (Table 1, runs 16–18). Since  $\text{HOOC-PEG-NH}_2$  was a zwitterion in aqueous solution, the pH was adjusted to 10.7 using 1.0 N NaOH in order to deprotonate the PEG terminal amines ( $\text{p}K_a = 10.4$ ). The size of the obtained nanospheres was 210–380 nm (Figure 1d) and decreased upon increasing the molecular weight of the PEG macroinitiators. To confirm the anionic charge assigned to the carboxyl group on the surface of the nanosphere, the  $\zeta$ -potential of the peptide nanospheres was measured in 0.001 M KCl solution at 25 °C. The  $\zeta$  potential of the nanospheres of runs 16, 17, and 18 from Table 1 were –34, –19, and –17 mV, respectively, clearly indicating the presence of anionic charges on the surface of the nanospheres. The molecular weight of the two components, the Phe homopolymer and p(Phe-*b*-EG), was estimated at  $M_w = 6060$  (DP = 41) and 17 590 (DP = 106), respectively, in our previous report using gel permeation chromatography (GPC) measurements.<sup>22</sup> However, detailed studies on the  $^1\text{H}$  NMR and MALDI-TOF mass of the component polymers resulted in a  $M_w = 2000$  (DP = 13) for the Phe homopolymer and  $M_w = 3000$  (DP = 7.4) for p(Phe-*b*-EG) in the peptide nanospheres (Table 1, run 4). A detailed

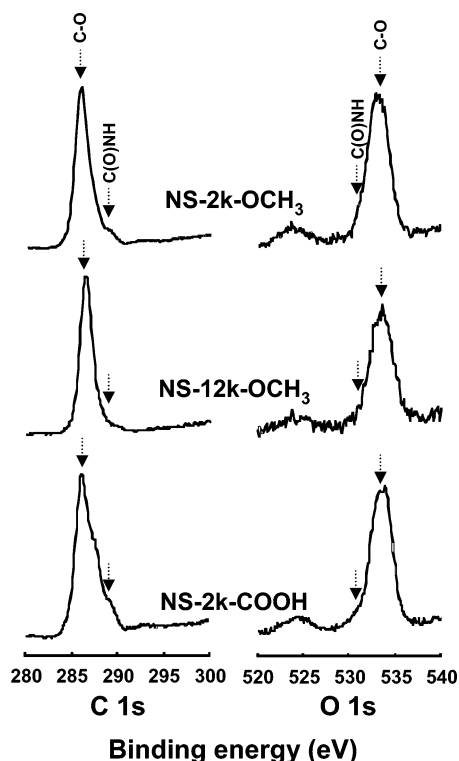


**Figure 2.** ESCA spectra in the region of the carbon and oxygen elements of peptide nanospheres of NS-2K-OCH<sub>3</sub> (Table 1, run 4), NS-12K-OCH<sub>3</sub> (Table 1, run 14), and NS-2K-COOH (Table 1, run 16).

discussion of the molecular weight is shown in the Supporting Information.

**Structural Analyses of the Peptide Nanospheres.** We investigated the structures of the peptide nanospheres by ESCA, <sup>1</sup>H NMR, FT-IR, and XRD measurements. ESCA analysis is a powerful method to confirm the chemical bonds on the nanosphere surface at ~10 nm of measurement depth. Figure 2 shows the ESCA spectra of three representative peptide nanospheres synthesized with various initiators: NS-2K-OCH<sub>3</sub> (NH<sub>2</sub>-PEG-OCH<sub>3</sub> with  $M_w = 2000$ ; Table 1, run 4), NS-12K-OCH<sub>3</sub> (NH<sub>2</sub>-PEG-OCH<sub>3</sub> with  $M_w = 12\,000$ ; Table 1, run 14), and NS-2K-COOH (NH<sub>2</sub>-PEG-COOH with  $M_w = 2000$ ; Table 1, run 16). An assignment of the ESCA spectra was referred to Huang's report.<sup>26</sup> A distinct O 1s peak at around 532.8 eV assigned to the ether oxygen of the PEG segments, and a C 1s peak at around 286.5 eV assigned to the ether carbon of the PEG segments or the  $\alpha$ -carbon of the Phe units, were observed in all nanospheres. However, an O 1s peak at around 531.3 eV assigned to the amide oxygen of the Phe units and C 1s peaks at around 285.0 and 288.0 eV assigned to the aliphatic, aromatic, and amide carbons of the Phe units were barely observed. These results suggest that PEG chains accumulated on the surface of the peptide nanospheres, indicating a core–corona structure composed of a hydrophobic core, mainly PPhe segments, and a hydrophilic corona layer, mainly PEG chains. In the case of NS-12K-OCH<sub>3</sub>, the peak intensity of the C 1s peak at 288.0 eV assigned to the amide carbon of the Phe segments was lower than that of NS-2K-OCH<sub>3</sub>, suggesting a thicker corona layer for NS-12K-OCH<sub>3</sub> depending on the higher molecular weight of the PEG macroinitiator.

The number of PEG chains on a single peptide nanosphere was determined by <sup>1</sup>H NMR measurements in D<sub>2</sub>O.<sup>27</sup> We estimated the number of PEG chains on the surface of the peptide nanospheres, NS-2K-OCH<sub>3</sub>, NS-2K-COOH, NS-3.4K-COOH (Table 1, run 17), and NS-4.5K-COOH (Table 1, run

18), per the unit mass from the intensity of the PEG methylene peak in the region of 3.5–3.7 ppm as compared with the methyl proton peak of DSS at 0 ppm. The size (as determined by DLS measurements) and density (assumed to be 1.05 g/cm<sup>3</sup>) of the nanospheres, the number of PEG chains on a single peptide nanosphere ( $N(\text{PEG})_{\text{surface}}$ ), the area occupied by a single PEG molecule ( $A_{\text{PEG}}$ ), and the average distance between PEG molecules ( $D_{\text{PEG}}$ ) were calculated. The results are summarized in Table 2. Here, the radius of gyration of PEG ( $R_g$ ) with  $M_w = 2000, 3400$ , and  $4500$  based on random coil models was calculated as 1.6, 2.1, and 2.6 nm by the following equation.<sup>28</sup>

$$R_g = 0.181N^{0.58} \text{ (nm)}$$

The average distances between PEG chains on the surface of the peptide nanospheres were calculated to be at least 3.2, 4.2, and 5.2 nm on the basis of the assumption of a mushroom conformation of PEG molecules. On the other hand, the  $D_{\text{PEG}}$  of NS-2K-OCH<sub>3</sub>, NS-2K-COOH, NS-3.4K-COOH, and NS-4.5K-COOH estimated from the <sup>1</sup>H NMR measurement had lower values, 0.75, 0.74, 1.1, and 2.2 nm, respectively, suggesting a brush conformation for the PEG chains on the surface of the peptide nanospheres. The PEG densities ( $\sigma_{\text{PEG}}$ ) were estimated to be 1.8 (NS-2K-OCH<sub>3</sub>), 1.8 (NS-2K-COOH), 0.91 (NS-3.4K-COOH), and 0.21 (NS-4.5K-COOH) chains/nm<sup>2</sup> from the  $N(\text{PEG})_{\text{surface}}$  and surface area. These graft densities corresponded to a high density regime rather than a moderate density regime, whose typical density was reported as 0.001–0.05 chains/nm<sup>2</sup>.<sup>16,17</sup> It was believed that particles with high-density polymer brushes can be generated only by surface-initiated living radical polymerization involving multiple steps.<sup>19–21</sup> To the best of our knowledge, this is the first example of a biodegradable peptide nanosphere with high-density polymer brushes.

To clarify the mechanism responsible for the high-density PEG chains on the peptide nanospheres, we investigated the secondary structure of the peptide nanosphere by FT-IR measurements in D<sub>2</sub>O (Figure 3). The FT-IR spectrum of the peptide nanosphere shows peaks at 1280, 963, 844, and 828 cm<sup>−1</sup> assigned to typical crystalline PEG,<sup>29–31</sup> indicating partial crystallinity of the PEG chain on the peptide nanospheres. In addition, the peaks of amide I at 1694 and 1630 cm<sup>−1</sup> and the peaks of amide II at 1541–1544 cm<sup>−1</sup> suggested a  $\beta$ -strand conformation of PPhe and p(Phe-*b*-EG) in the peptide nanospheres on the basis of Hilderson's report.<sup>32</sup> We pursued the secondary structure of the peptide nanospheres during the polymerization process. Polymerization was performed in D<sub>2</sub>O/DMSO-*d*<sub>6</sub> mixed solvents instead of H<sub>2</sub>O/DMSO in order to avoid overlap between the H<sub>2</sub>O and amide I peaks. Figure 4a shows the FT-IR spectra of nanospheres prepared for various reaction times: 0.5, 1, 2, 8, and 24 h. Hilderson et al. reported that amide I' peaks at 1653–1658, 1640–1642, and 1622–1633 cm<sup>−1</sup> in D<sub>2</sub>O could be assigned to unordered,  $\alpha$ -helix, and  $\beta$ -strand conformations, respectively.<sup>32</sup> The composition ratio of each conformation was estimated by peak fitting software (GRAMS/AI ver.7, Thermo Galactic). Figure 4b shows the relationship between the composition percentage of each conformation and the reaction time. The  $\beta$ -strand conformation was slightly decreased in the initial stage of polymerization and saturated at 75% after 2 h. Both unordered and  $\alpha$ -helix conformations were saturated at ~15% after 2 h of polymerization. It is known that a phenylalanine homopolymer with more than 12 repeating units easily transforms from a  $\beta$ -form to an  $\alpha$ -helix conformation during polymerization.<sup>33</sup> However, conformational transition from  $\beta$ -form to  $\alpha$ -helix of the PPhe and

Table 2. Structure of the Peptide Nanospheres

|  | NS-2K-OCH <sub>3</sub> | NS-2K-COOH         | NS-3.4K-COOH       | NS-4.5K-COOH       |
|--|------------------------|--------------------|--------------------|--------------------|
| size (nm)                                    | 430                    | 380                | 340                | 210                |
| $N(\text{PEG})_{\text{surface}}^a$           | $1.0 \times 10^6$      | $0.83 \times 10^6$ | $0.32 \times 10^6$ | $0.29 \times 10^6$ |
| $A_{\text{PEG}} (\text{nm}^2)^b$             | 0.56                   | 0.55               | 1.1                | 4.8                |
| $D_{\text{PEG}} (\text{nm})^c$               | 0.75                   | 0.74               | 1.1                | 2.2                |
| $D_{\text{PEG}}/2R_g^d$                      | 0.23                   | 0.23               | 0.26               | 0.42               |
| $\sigma_{\text{PEG}} (\text{chains/nm}^2)^e$ | 1.8                    | 1.8                | 0.91               | 0.21               |

<sup>a</sup>  $N(\text{PEG})_{\text{surface}}$  means the number of PEG chain on a single peptide nanosphere surface.  $N(\text{PEG})_{\text{surface}}$  was estimated by <sup>1</sup>H NMR spectrum in D<sub>2</sub>O using DSS as reference. <sup>b</sup>  $A_{\text{PEG}}$  means the occupied area by 1 PEG molecule. Surface area of peptide nanospheres was divided by  $N(\text{PEG})_{\text{surface}}$ . <sup>c</sup>  $D_{\text{PEG}}$  means the average distance between PEG chains on the surface, square root of  $A_{\text{PEG}}$ . <sup>d</sup>  $R_g$  means the radius of gyration of PEG. <sup>e</sup>  $\sigma_{\text{PEG}}$  means the surface density of PEG.

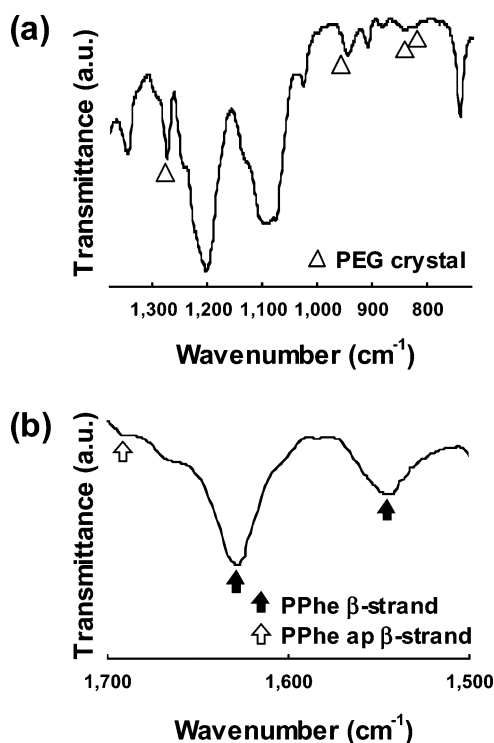


**Figure 3.** FT-IR spectra of the peptide nanospheres in D<sub>2</sub>O. The triangles represent the peaks assigned to PEG crystals (a). The solid and open arrows represent the peaks assigned to PPhe  $\beta$ -strands and PPhe antiparallel (ap)  $\beta$ -strands, respectively (b).

Phe segment of p(Phe-*b*-EG) in these peptide nanospheres was barely observed.

To investigate the crystal structures of the peptide nanosphere components, we performed wide-angle X-ray diffraction (WAXD) measurements. Figure 5 shows WAXD diagrams of the NH<sub>2</sub>-PEG-COOH initiator ( $M_w = 2000$ ), poly(phenylalanine) synthesized with a solitary *n*-butylamine (Table 1, run 1), and the peptide nanosphere (Table 1, run 16; NS-2K-COOH). All samples were measured in powder conditions. NS-2K-COOH showed a distinct peak, indicating that this component of the peptide nanosphere formed a crystalline structure at the molecular level. A strong diffraction appeared at  $2\theta = 18.7^\circ$  ( $d_3$ ) for PPhe and NS-2K-COOH ( $\theta$  = diffraction angle), corresponding to a spacing of 0.47 nm, suggesting a hydrogen-bond distance in a  $\beta$ -sheet crystalline structure as described in Pochan's report.<sup>34</sup> Diffraction peaks at  $2\theta = 7.1^\circ$  ( $d_1$ ),  $14.6^\circ$  ( $d_2$ ), and  $22.0^\circ$  ( $d_5$ ) for NS-2K-COOH corresponded to spacing of 1.24, 0.61, and 0.40 nm, respectively. These reflections seem to describe a relationships of  $d_1:d_2:d_5 = d_1:d_1/2:d_1/3$ , indicating a layered structure with a thickness of 1.24 nm because of the intersheet stacking periodicity.<sup>34</sup> Furthermore, the diffractions at  $2\theta = 19.2^\circ$  ( $d_4$ ) and  $23.0^\circ$  ( $d_6$ ) for NH<sub>2</sub>-PEG-COOH and NS-2K-COOH were assigned to PEG crystals.<sup>35</sup> The crystalline

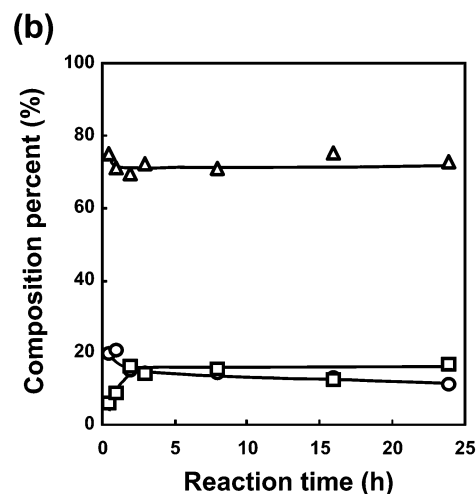
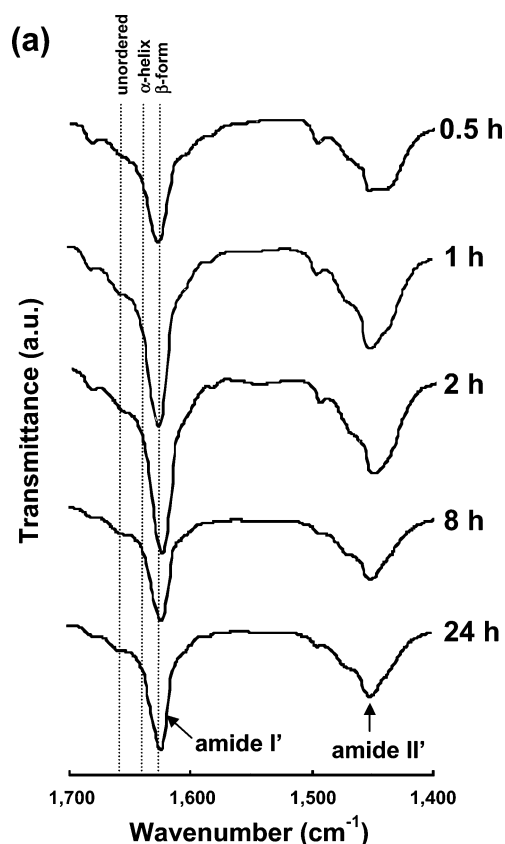


**Figure 4.** (a) FT-IR spectra of peptide nanospheres obtained after various reaction times (0.5, 1, 2, 8, and 24 h). The relationship between the composition percentage of each conformation and the reaction time (b). The circles, triangles, and open squares indicate the  $\alpha$ -helix,  $\beta$ -strand, and unordered conformations, respectively.

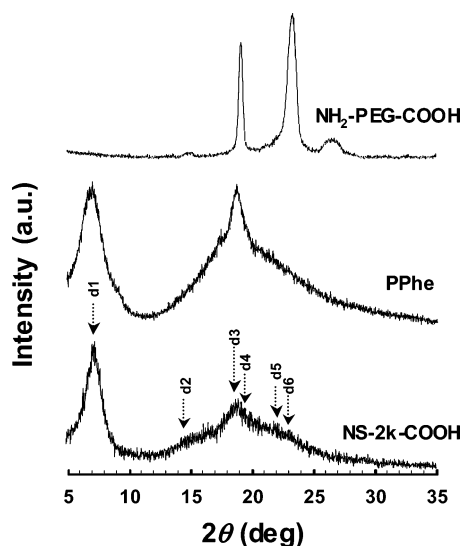


**Figure 5.** Wide-angle X-ray diffraction (WAXD) diagrams of  $\text{NH}_2\text{-PEG-COOH}$  ( $M_w = 2000$ ), poly(phenylalanine) synthesized with a solitary *n*-butylamine (Table 1, run 1), and the peptide nanospheres of NS-2K-COOH (Table 1, run 16).

**Table 3. Proteins Used in This Study**

| protein             | $M_w$ (kDa) <sup>a</sup> | pI   | $h \times w \times l$ (nm) <sup>b</sup> |
|---------------------|--------------------------|------|---|
| OVA                 | 45                       | 4.6  | $7.0 \times 2.5 \times 2.5$             |
| BSA                 | 69                       | 4.8  | $14 \times 4.0 \times 4.0$              |
| lysozyme            | 14                       | 11.1 | $4.5 \times 3.0 \times 3.0$             |
| cytochrome <i>c</i> | 13                       | 10.2 | $3.7 \times 2.5 \times 2.5$             |

<sup>a</sup> Molecular weight of the proteins. <sup>b</sup> Approximate molecular dimension of the proteins.

**Table 4. Protein Adsorption on the Surface of Peptide Nanospheres**

| protein             | NS-2K-OCH <sub>3</sub>                   |                           | NS-2K-COOH                               |                           |
|---------------------|--|---------------------------|--|---------------------------|
|                     | protein adsorption (ng/cm <sup>2</sup> ) | coverage (%) <sup>a</sup> | protein adsorption (ng/cm <sup>2</sup> ) | coverage (%) <sup>a</sup> |
| OVA                 | 50                                       | 4                         | n.d. <sup>b</sup>                        |                           |
| BSA                 | 110                                      | 15                        | n.d. <sup>b</sup>                        |                           |
| lysozyme            | n.d. <sup>b</sup>                        |                           | n.d. <sup>b</sup>                        |                           |
| cytochrome <i>c</i> | n.d. <sup>b</sup>                        |                           | n.d. <sup>b</sup>                        |                           |

<sup>a</sup> Surface coverage of the proteins was estimated from molecular dimension of each protein described in Table 3. <sup>b</sup> n.d. = not detected.

structures of the  $\beta$ -sheet and PEG also supported the FT-IR spectra.

From the results of the FT-IR and WAXD measurements, the high-density PEG chains of these peptide nanospheres seem to be caused by the  $\beta$ -sheet crystalline structure of the PPhe and Phe segments of p(Phe-*b*-EG).

**Physical Adsorption or Chemical Immobilization of Proteins onto the Peptide Nanospheres.** To evaluate the stealth properties against nonspecific protein adsorption onto the peptide nanospheres, we performed protein adsorption experiments using NS-2K-OCH<sub>3</sub> and NS-2K-COOH. The peptide nanospheres were dispersed in PBS (pH 7.4) at 10 mg/mL and incubated with an equivalent volume of 4 mg/mL protein solution (PBS, pH 7.4) at 4 °C for 24 h. After washing with PBS, the amount of physically adsorbed proteins was detected by the ninhydrin method. Table 3 shows the isoelectric point, molecular weight, and round size of the proteins used in this study as model proteins,<sup>36–38</sup> and Table 4 shows the adsorption amount and surface coverage of each protein. The amount of adsorbed ovalbumine (OVA) and bovine serum albumin (BSA) onto NS-2K-OCH<sub>3</sub> was 50 ng/cm<sup>2</sup> (coverage = 3%) and 110 ng/cm<sup>2</sup>

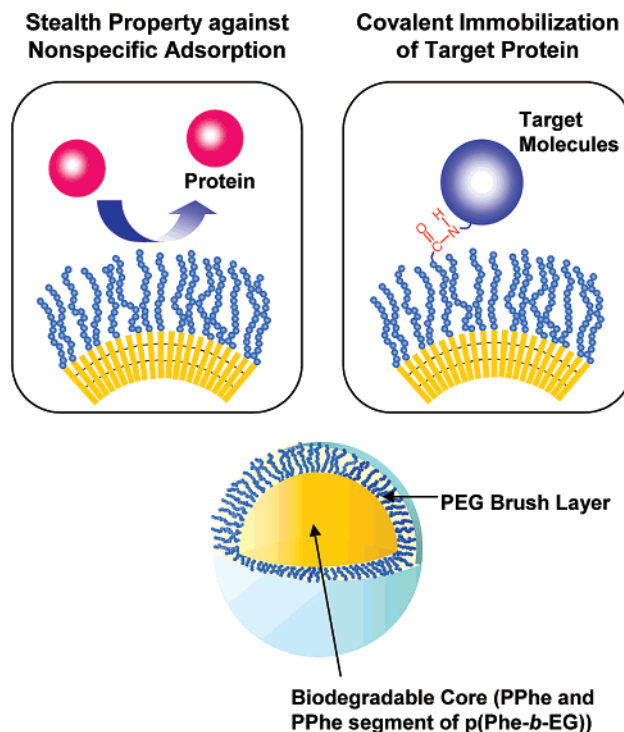


**Figure 6.** Schematic illustration of the stealth properties against nonspecific protein adsorption and the covalent immobilization of target proteins on the peptide nanospheres with carboxyl groups.

(coverage = 15%), respectively, and adsorption of lysozyme and cytochrome *c* onto NS-2K-OCH<sub>3</sub> were not observed. On the other hand, in the case of NS-2K-COOH, the nonspecific adsorption of these proteins was not observed. It is noted that adsorption of cytochrome *c* and lysozyme, having positive charge under the incubation conditions, onto both peptide nanospheres was not observed, even though NS-2K-COOH has a negative charge under the same conditions. Furthermore, for actual applications, the protein adsorption test was performed in Eagle's medium containing 10% fetal bovine serum at 4 °C for 24 h. The amount of nonspecific adsorbed serum proteins for NS-2K-COOH was estimated at only 24 ng/cm<sup>2</sup> (coverage = 3%) using a calibration curve for BSA. We evaluated the hemolytic activity of the peptide nanospheres (Table 1, run 17) using red blood cells (RBCs) under various pH conditions at 37 °C for 1 h. No hemolysis was observed at any pH (Supporting Information). These results indicated the stealth properties of the peptide nanospheres were caused by the high-density PEG brushes. We performed the covalent immobilization of OVA as a model protein onto NS-2K-COOH via amide bond formation with a condensation reagent, WSC. The amount of immobilized OVA for NS-2K-COOH through covalent bonding between the carboxyl group of the hydrophilic corona layers and the amino group of the proteins was ~15 ng/cm<sup>2</sup>, whereas the nonspecific adsorption of OVA was not detected by the ninhydrin method. Furthermore, physical adsorption of OVA, BSA, lysozyme, and cytochrome *c* onto the OVA-immobilized NS-2K-COOH was not observed. Figure 6 summarizes the stealth properties against nonspecific protein adsorption and covalent immobilization of the target proteins. Our peptide nanospheres possessed both possible stealth properties and chemical functionality and may represent a novel class of biodegradable and biocompatible nanospheres.



## Conclusions

Peptide nanospheres with PEG brushes were prepared by the one-step polymerization of Phe-NCA with the dual initiators of hydrophobic *n*-butylamine and hydrophilic NH<sub>2</sub>-PEG-OCH<sub>3</sub> or NH<sub>2</sub>-PEG-COOH. <sup>1</sup>H NMR measurements of the peptide nanospheres showed that the PEG chain adopted a brush conformation. The FT-IR and WAXD analyses revealed a  $\beta$ -strand conformation for the PPhe and Phe segments of p(Phe-*b*-EG) triggered the high-density PEG brush conformation in the corona layer of the peptide nanospheres. Experiments investigating protein adsorption and immobilization onto the nanosphere surface suggested the possibility of stealth properties and chemical functionality. In vivo studies on the stealth properties of these peptide nanospheres are now in progress. Peptide nanospheres with PEG brushes are expected to be useful as a novel biodegradable nanosphere in the biomedical fields.

**Acknowledgment.** This research was supported by Core Research for Evolutional Science and Technology (CREST) from the Japan Science and Technology Agency (JST). This study was also supported by the Center of Excellence (COE) Program for the 21st Century, Osaka University. We acknowledge Mr. Ohzono, a technician of Kagoshima University, for ESCA studies and Dr. Akagi, a researcher of CREST-JST, for the hemolytic activity test.

**Supporting Information Available:** Detailed data of <sup>1</sup>H NMR, MALDI-TOF mass measurements, and hemolytic activity tests. This material is available free of charge via the Internet at <http://pubs.acs.org>.

## References and Notes

- (1) Kataoka, K.; Harada, A.; Nagasaki, Y. *Adv. Drug Delivery Rev.* **2001**, *47*, 113–131.
- (2) Cho, C. S.; Cho, K. Y.; Park, I. K.; Kim, S. H.; Sagawa, T.; Uchimura, M.; Akaike, T. *J. Controlled Release* **2001**, *77*, 7–15.
- (3) Choi, Y. C.; Kim, S. Y.; Moon, M. H.; Kim, S. H.; Lee, K. S.; Byun, Y. *Biomaterials* **2001**, *22*, 995–1004.
- (4) Suslick, K. S.; Grinstaff, M. W. *J. Am. Chem. Soc.* **1990**, *112*, 7807–7809.
- (5) Bellomo, E. G.; Wyrsta, M. D.; Pakstis, L.; Pochan, D. J.; Deming, T. J. *Nat. Mater.* **2004**, *3*, 244–248.
- (6) Reches, M.; Gazit, E. *Nano Lett.* **2004**, *4*, 581–585.
- (7) Matsuura, K.; Murasato, K.; Kimizuka, N. *J. Am. Chem. Soc.* **2005**, *127*, 10148–10149.
- (8) Akashi, M.; Kirikihira, I.; Miyauchi, N. *Angew. Makromol. Chem.* **1985**, *132*, 81–89.
- (9) Serizawa, T.; Takehara, S.; Akashi, M. *Macromolecules* **2000**, *33*, 1759–1764.
- (10) Matsusaki, M.; Fuchida, T.; Kaneko, T.; Akashi, M. *Biomacromolecules* **2006**, *6*, 2374–2379.
- (11) Matsusaki, M.; Hiwatari, K.-i.; Higashi, M.; Kaneko, T.; Akashi, M. *Chem. Lett.* **2004**, *33*, 398–399.
- (12) Akagi, T.; Higashi, M.; Kaneko, T.; Kida, T.; Akashi, M. *Biomacromolecules* **2006**, *7*, 297–303.
- (13) Itoh, Y.; Matsusaki, M.; Kida, T.; Akashi, M. *Chem. Lett.* **2004**, *33*, 1552–1553.
- (14) Itoh, Y.; Matsusaki, M.; Kida, T.; Akashi, M. *Biomacromolecules* **2006**, *7*, 2715–2718.
- (15) Yokoyama, M.; Kwon, S. G.; Okano, T.; Sakurai, Y.; Seto, T.; Kataoka, K. *Bioconjugate Chem.* **1992**, *3*, 295–301.
- (16) Yamamoto, S.; Ejaz, M.; Tujii, Y.; Matsumoto, M.; Fukuda, T. *Macromolecules* **2000**, *33*, 5602–5607.
- (17) Yamamoto, S.; Ejaz, M.; Tujii, Y.; Fukuda, T. *Macromolecules* **2000**, *33*, 5608–5612.
- (18) Yoshikawa, C.; Goto, A.; Tujii, Y.; Fukuda, T.; Kimura, T.; Yamamoto, K.; Kishida, A. *Macromolecules* **2006**, *39*, 2284–2290.
- (19) Ohno, K.; Morinaga, T.; Koh, K.; Tujii, Y.; Fukuda, T. *Macromolecules* **2005**, *38*, 2137–2142.
- (20) Ohno, K.; Morinaga, T.; Takeno, S.; Tujii, Y.; Fukuda, T. *Macromolecules* **2006**, *39*, 1245–1249.
- (21) Li, D.; Sheng, X.; Zhao, B. *J. Am. Chem. Soc.* **2005**, *127*, 6248–6256.
- (22) Matsusaki, M.; Waku, T.; Kaneko, T.; Kida, T.; Akashi, M. *Langmuir* **2006**, *22*, 1396–1399.
- (23) Bronich, K. T.; Keifer, A. P.; Shlyakhtenko, S. L.; Kabanov, V. A. *J. Am. Chem. Soc.* **2005**, *127*, 8236–8237.
- (24) Daly, W. H.; Poche, D. *Tetrahedron Lett.* **1988**, *29*, 5859–5862.
- (25) Kurita, K.; Yoshida, A.; Koyama, Y. *Macromolecules* **1988**, *21*, 1579–1583.
- (26) Huang, N.-P.; Michel, R.; Voros, J.; Textor, M.; Hofer, R.; Rossi, A.; Elbert, L. D.; Hubbell, A. J.; Spencer, D. N. *Langmuir* **2001**, *17*, 489–498.
- (27) Kawaguchi, S.; Winnik, A. M.; Ito, K. *Macromolecules* **1996**, *29*, 4465–4472.
- (28) Pasche, S.; De Paul, S. M.; Vörös, J.; Spencer, D. N.; Textor, M. *Langmuir* **2003**, *19*, 9216–9225.
- (29) Yoshihara, T.; Tadokoro, H.; Murahashi, S. *J. Chem. Phys.* **1964**, *41*, 2902–2911.
- (30) Shimomura, M.; Tanabe, Y.; Watanabe, Y.; Kobayashi, M. *Polymer* **1990**, *31*, 1441–1448.
- (31) Dissanayake, M. A. K. L.; Frech, R. *Macromolecules* **1995**, *28*, 5312–5319.
- (32) Hilderson, J. H.; Ralston, B. G. In *Subcellular Biochemistry*; Goormaghtigh, E.; Cabiaux, V.; Ruysschaert, J.-M., Eds.; Plenum Press: New York, 1994; Vol. 23, pp 329–450.
- (33) Kricheldorf, H. R. *Makromol. Chem.* **1983**, *184*, 1407–1421.
- (34) Lamm, M. S.; Rajagopal, K.; Schneider, J. P.; Pochan, D. J. *J. Am. Chem. Soc.* **2005**, *127*, 16692–16700.
- (35) Kaneko, T.; Tanaka, S.; Ogura, A.; Akashi, M. *Macromolecules* **2005**, *38*, 4861–4867.
- (36) Sigal, B. G.; Mrksick, M.; Whitesides, M. G. *J. Am. Chem. Soc.* **1998**, *120*, 3464–3473.
- (37) Dickerson, E. R.; Kopka, L. E.; Weinzierl, J.; Varnum, J.; Eisenberg, D.; Margoliash, E. *J. Biol. Chem.* **1967**, *242*, 3015–3018.
- (38) Johnson, E. J.; Matijetic, E. *Colloid Polym. Sci.* **1992**, *270*, 353–363.

MA0707638